



Spin susceptibility in superconducting LiFeAs studied by polarized neutron diffraction

J. Brand,¹ A. Stunault,² S. Wurmehl,^{3,4} L. Harnagea,³ B. Büchner,^{3,4} M. Meven,^{5,6} and M. Braden^{1,*}

¹*II. Physikalisches Institut Universität zu Köln Zülpicher Str. 77, D-50937 Köln, Germany*

²*Institut Laue-Langevin, B.P. 156, 6 rue Jules Horowitz, F-38042 Grenoble Cedex 9, France*

³*Leibniz-Institut für Festkörper- und Werkstoffforschung Dresden, Helmholtzstrasse 20, D-01069 Dresden, Germany*

⁴*Institut für Festkörperforschung, Technische Universität Dresden, D-01171 Dresden, Germany*

⁵*Institut für Kristallographie, Outstation at MLZ, Lichtenbergstr. 1, 85748 Garching, Germany*

⁶*Jülich Centre for Neutron Science, Forschungszentrum Jülich GmbH, Outstation at MLZ, Lichtenbergstr. 1, 85748 Garching, Germany*

(Received 15 November 2013; revised manuscript received 9 January 2014; published 30 January 2014)

The local spin susceptibility in superconducting LiFeAs was studied by polarized neutron diffraction as a function of temperature. In the superconducting phase the spin susceptibility is clearly suppressed and it can be well described by the Yosida function suggesting a singlet pairing to occur at low temperature. The spin susceptibility in the normal state and its suppression in the superconducting phase are fully comparable to observations in Co-doped BaFe₂As₂.

DOI: 10.1103/PhysRevB.89.045141

PACS number(s): 74.25.-q, 74.70.Xa, 75.25.-j

I. INTRODUCTION

The FeAs-based superconductors continue attracting interest, not only due to their high T_c values, up to 55 K [1–3], but also due to the unconventional nature of the superconductivity, which always appears near a magnetically ordered phase [4]. A close connection between the magnetism and the superconducting pairing mechanism thus seems very likely. In most FeAs-based families superconductivity is induced either by chemical doping or by application of high pressure on a stoichiometric parent phase which exhibits a structural distortion and antiferromagnetic ordering at low temperatures [5–7]. LiFeAs is the only exception, as it exhibits superconductivity at elevated temperatures without doping and at ambient pressure [8–10].

LiFeAs crystallizes in the tetragonal space group $P4/nmm$ with lattice constants $a = 3.7914(7)$ Å and $c = 6.364(2)$ Å at room temperature [8]. The unit cell consists of FeAs layers which are separated by a double layer of Li Atoms. So far, there is no experimental indication for the structural or for the magnetic phase transitions that appear in the other FeAs parent materials [10,16]; instead, single crystals of LiFeAs exhibit superconductivity below $T_c \approx 18$ K [8–10].

It remains an open question whether the ambient pressure superconductivity in stoichiometric LiFeAs possesses the same character as that in the other FeAs-based compounds. ARPES experiments on LiFeAs indicate weaker nesting between hole and electron Fermi surfaces due to shallow hole bands [11,12]. The first de Haas-van Alphen measurement only detected a few electron Fermi surfaces, in rough agreement with simple band-structure calculations [13], but more recent de Haas-van Alphen studies confirmed the ARPES results concerning the hole pockets [14]. Only by taking electronic correlations into account can band-structure calculations reproduce the proper shape of the hole Fermi surfaces in LiFeAs [12,15]. Single-crystal inelastic neutron scattering studies still find substantial antiferromagnetic correlations near the corresponding wave vector [16] and no evidence of

an eminent ferromagnetic instability. The antiferromagnetic correlations show a transverse incommensurate modulation similar to calculations and observations for electron-doped BaFe₂As₂ [17,18] and in agreement with the peculiar shape of the hole Fermi surfaces in LiFeAs compared to the other FeAs parent compounds. The strong elongation of the FeAs₄ tetrahedra in the c direction combined with the electronic correlations seems to imply an important orbital rearrangement [12,16]. Nonstoichiometric LiFeAs, however, exhibits evidence of a ferromagnetic ordering [19–21] that has no counterpart in the other families so far. Support for another pairing symmetry was deduced from NMR Knight-shift experiments [22] and from quasiparticle interference [23], inspiring the theoretical proposal of triplet pairing associated with either ferromagnetic fluctuations [24] or small- q phonons [25].

Triplet and singlet superconducting pairing can be easily distinguished by measurements of the spin susceptibility. While the susceptibility is fully suppressed for singlet pairing, finite susceptibility remains along particular directions in the case of triplet pairing. Due to superconducting shielding the spin susceptibility cannot be measured with macroscopic techniques in the superconducting state, but NMR Knight-shift and polarized neutron-diffraction experiments can isolate these contributions. In the context of triplet superconductivity, Sr₂RuO₄ is a well-studied unconventional superconductor for which both Knight-shift and neutron measurements find a nonvanishing spin susceptibility that does not change across the superconducting transition, consistent with triplet pairing [26,27]. In contrast, the superconductor V₃Si [28] shows a diminishing spin susceptibility indicating singlet pairing. Also, the unconventional superconductors UPt₃, UBe₁₃, and CeCu₂Si₂ [29] as well as YBa₂Cu₃O_{7-x} [30] were studied with the polarized-neutron diffraction technique, and a constant and a suppressed spin susceptibility were found in the former and in the latter cases, respectively.

Baek *et al.* [22], measured the Knight shift of the ⁷⁵As nuclear magnetic resonance. They apply a magnetic field of 7 T parallel and perpendicular to the crystallographic c axis. The results show no change in the Knight shift upon going below the transition temperature when the field is exactly parallel to the a,b planes. This experiment was interpreted as evidence

*braden@ph2.uni-koeln.de

of an odd-wave spin-triplet pairing. In other FeAs-based superconductors Knight-shift experiments [31–34] indicate singlet pairing, as well as a polarized neutron-diffraction study on Co-doped BaFe₂As₂ [35].

Here, we present results of polarized and unpolarized neutron-diffraction experiments on single-crystalline LiFeAs. There is no indication of a structural phase transition, but we observe clear suppression of spin susceptibility across the superconducting transition that is characteristic of singlet pairing.

II. EXPERIMENTAL RESULTS AND DISCUSSION

Three crystals of different growth processes were used in our studies. The crystal for determination of the nuclear structure was grown with natural Li, while for the polarized experiments the less-absorbing ⁷Li isotope was used. Details on the crystal growth with a self-flux technique and typical characterization can be found in [36]. LiFeAs is very air sensitive, therefore special care was taken to avoid any contact with air. All crystals were mounted in a glove box on an aluminum can that contained either argon or helium. These cans were then mounted on diffractometers.

To examine the crystal structure of LiFeAs at low temperatures we measured sets of Bragg reflections at 25 and at 2 K using the hot-neutron four-circle diffractometer HEIDI operated by RWTH Aachen/FZ Jülich [Jülich Aachen Research Alliance (JARA)] at the Heinz Maier-Leibnitz Zentrum in Garching, Germany. Using a wavelength of 0.794 Å, 700 integrated Bragg-reflection intensities were determined at both temperatures and were merged into sets of 227 unique reflections, of which only a single reflection showed an intensity below three times its error. The statistical error bars of the measured structure factors were modified by $\sigma = [\sigma_{\text{stat}}^2 + (F_{\text{obs}} \cdot 0.01)^2 + 1]^{\frac{1}{2}}$, with σ_{stat} the statistical error and F_{obs} the observed structure factor, in order to take the extinction and multiple diffraction contaminations into account [37]. Data were numerically corrected for absorption and an anisotropic extinction correction with the secondary-extinction Becker-Coppens model was applied during the refinements, which were performed using the Prometheus program package. The results of the structure refinements in space group *P4/nmm* with the 227 independent reflections at 25 and 2 K, are listed in Table I. There is no significant difference between crystal

TABLE I. Atomic positions of LiFeAs at 25 and at 2 K determined by single-crystal neutron diffraction. Sets of 227 unique reflection intensities were used to refine the structure at 25 and at 2 K, yielding R values of $R_{w\text{-int}} = 8.6/R_{u\text{-int}} = 6.4\%$ and $R_{w\text{-int}} = 8.7/R_{u\text{-int}} = 6.7\%$, respectively.

Atom	<i>T</i> (K)	<i>x</i>	<i>y</i>	<i>z</i>	<i>U</i> ₁₁	<i>U</i> ₃₃
Li	25	0.25	0.25	0.6552(9)	0.0106(15)	0.0098(22)
	2	0.25	0.25	0.6552(9)	0.0107(15)	0.0111(23)
Fe	25	0.75	0.25	0	0.0028(2)	0.0058(3)
	2	0.75	0.25	0	0.0028(2)	0.0058(3)
As	25	0.25	0.25	0.2359(2)	0.0035(2)	0.0058(4)
	2	0.25	0.25	0.2359(2)	0.0033(2)	0.0058(4)

structures at the two studied temperatures and the data do not indicate any significant nonstoichiometry. The occupation of the Li site was refined to 0.98(5) at both temperatures; note that the relatively large error arises from the small scattering length of Li and from the sizable mosaic spread of the crystal. Our results agree perfectly with previous structure determinations at higher temperatures [8,36], indicating that there is no sizable change in the crystal structure of LiFeAs upon cooling. In addition, we recorded the intensities of several strong nuclear Bragg reflections between 2 K and room temperature. The structural phase transition occurring in the other stoichiometric FeAs compounds results in twining and, therefore, possesses a strong impact on the extinction conditions. In the case of doped BaFe₂As₂, even a weak orthorhombic distortion persisting at intermediate doping can thus easily be detected as an increase in diffraction intensity at strong nuclear Bragg peaks [38]. The absence of any anomaly in the temperature dependence of the strong Bragg intensities in LiFeAs underlines the absence of the orthorhombic distortion in this material.

In an unpolarized neutron-diffraction experiment the nuclear and magnetic intensities superpose, which makes it very difficult to detect a weak magnetic signal on top of the stronger nuclear peaks. In a polarized neutron experiment, however, the scattered intensity corresponds to the square of the sum of nuclear and magnetic structure factors, which allows for the detection of even small magnetic moments that are induced by an external magnetic field [40]:

$$\left(\frac{d\sigma}{d\Omega}\right)_{\text{NSF}} \propto \left| \frac{\gamma r_0}{2\mu_B} \cdot \sigma_i \cdot \mathbf{F}_M(\mathbf{G}) + \mathbf{F}_N(\mathbf{G}) \right|^2. \quad (1)$$

\mathbf{G} are the reciprocal lattice vectors, \mathbf{F}_N is the nuclear structure factor, and \mathbf{F}_M is the magnetic structure factor (the Fourier-transform coefficient of the magnetization in units of Bohr magnetons, of which only the component perpendicular to the scattering vector contributes). In Eq. (1) extinction effects and higher-order contaminations are neglected. σ_i symbolizes the initial neutron spin polarization, which is set parallel or antiparallel to the applied magnetic field. $\gamma = 1.913$ is the neutron gyromagnetic factor and r_0 is the classical Thomson radius; combination of both leads to $\gamma r_0 \sim 0.54 \times 10^{-12} \text{ cm}$ [39]. To isolate the magnetic scattering from the nuclear one we can measure the difference between the scattering of an “up” -polarized I_{\uparrow} and a “down” -polarized I_{\downarrow} neutron beam, the so-called “flipping ratios,” $R = \frac{I_{\uparrow}}{I_{\downarrow}}$. Reversing the neutron polarization reverses the magnetic contribution in Eq. (1). In the case of magnetization induced by an external magnetic field, which is parallel or antiparallel to the neutron polarization, this leads to

$$R = \frac{|F_N(\mathbf{G}) + (\gamma r_0/2\mu_B)F_{M\parallel}(\mathbf{G})|^2}{|F_N(\mathbf{G}) - (\gamma r_0/2\mu_B)F_{M\parallel}(\mathbf{G})|^2}, \quad (2)$$

with $F_{M\parallel}(\mathbf{G})$ the component of the magnetic structure factor perpendicular to the scattering vector. We recall that the magnetic scattering is supposed to arise entirely from the induced magnetization.

By combining the measured flipping ratios with the nuclear structure factors known from the unpolarized experiment one obtains the magnetic structure factors, from which one may deduce the magnetization density [40]. Flipping ratios in

LiFeAs were measured on the D3 diffractometer at the Institut Laue-Langevin in Grenoble. With this instrument one can generate a neutron beam with a polarization of $p = 94.5\%$ and a wavelength of $\lambda = 0.825 \text{ \AA}$ with the (111) Bragg position of a Heusler Cu₂MnAl monochromator.

To study the problem of whether LiFeAs is a spin-singlet or a triplet superconductor, we measured flipping ratios at different temperatures above and below the superconducting transition. Note that $T_C \approx 18 \text{ K}$ without an applied magnetic field but that the transition occurs at a lower temperature in a high magnetic field. We choose different Bragg reflections with a high predicted flipping ratio, (110) and (002), and first applied an external field of 9 T parallel to the [1-10] direction. The rather high field of 9 T is needed in these experiments in order to induce magnetic polarization sufficient to result in satisfying counting statistics. With the nuclear structure we may transform the flipping ratios into magnetic structure factors. If one further assumes that magnetization is entirely located at the Fe ions, and neglecting the Debye-Waller and form factors at these low Q values, these paramagnetic structure factors directly correspond to the magnetization per cell (two formula units) at both reflections, as there is full interference of the Fe sites at these two reflections. However, the finite diamagnetic contributions and a more complex spin-density distribution already cause deviation between the F_M and the total magnetization. The results are shown in Fig. 1 as diamonds.

At the top in Fig. 1 the magnetic structure factors of the (110) and the (002) Bragg reflections (in μ_B/cell) are plotted against the temperature. At the bottom of this figure the average of these two magnetic moments is shown. The behavior of the spin susceptibility for singlet superconductors can be well described with the Yosida function [41],

$$Y(T) = \frac{\chi}{\chi_N} = \frac{F_{M\parallel}(T)}{F_{M\parallel}(T > T_c)} = \frac{\beta}{\Delta} \left(\frac{\frac{d\Delta}{d\beta}}{1 + \frac{\beta}{\Delta} \frac{d\Delta}{d\beta}} \right), \quad (3)$$

with $\beta = 1/k_B T$, where Δ is the energy gap and χ_N stands for the normal value of the susceptibility. Einzel [42] examines the Yosida function for temperatures near T_C and for $T \rightarrow 0$ and deduces the single equation:

$$Y(T) = \sqrt{\frac{2\pi\Delta}{k_B T}} e^{-\frac{\Delta}{k_B T}} \left(1 + \frac{3 k_B T}{8 \Delta} \right) \left(1 - \left(\frac{T}{T_c} \right)^\kappa \right) + e^{\Delta(\frac{1}{k_B T_c} - \frac{1}{k_B T})} \left(\frac{T}{T_c} \right)^{\kappa - \frac{1}{2}}, \quad (4)$$

$$\kappa = \frac{\left(\frac{5}{2} - \frac{\Delta}{K_B T_c} \right)}{\left(1 - \sqrt{\frac{2\pi\Delta}{k_B T_c} e^{-\frac{\Delta}{k_B T_c}}} \left(1 + \frac{3 k_B T_c}{8 \Delta} \right) \right)}. \quad (5)$$

The spin susceptibility clearly drops at the superconducting transition, indicating a singlet pairing for a magnetic field parallel to the a, b planes. However, the spin susceptibility does not fully disappear at low temperatures. This behavior occurs also in other superconductors like V₃Si and Ba(Fe_{1-x}Co_x)₂As₂ ($x = 0.065$) [26,28,35]. The origins of this residual value are the van Vleck part of the susceptibility [43] and the spin susceptibility in the vortex cores arising from the high field

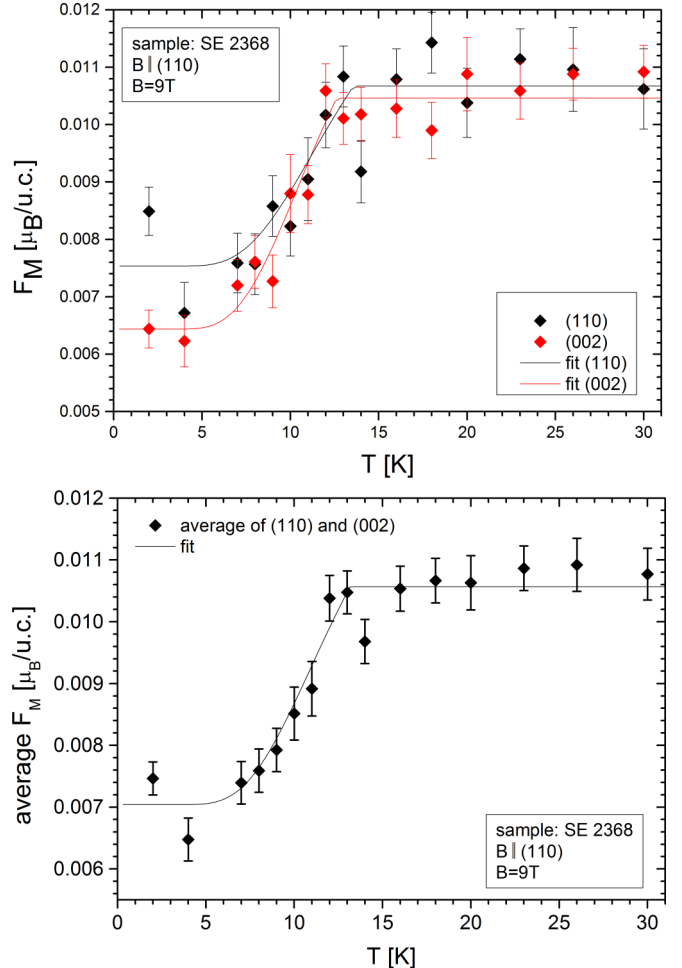


FIG. 1. (Color online) Magnetic moments of LiFeAs with an applied field of 9 T parallel to the [1-10] direction. Top: Moments of the (110) and the (002) Bragg reflection. Bottom: The average of both. Solid lines are fits of the Yosida function [41].

of our measurement, χ_{res} . This additional term leads to the equation

$$F_M(T) \propto H \cdot \chi = H(\chi_N \cdot Y(T) + \chi_{\text{res}}). \quad (6)$$

The solid lines in Fig. 1 represent such a Yosida fit. The behavior of the magnetic moments can be well described by this function. The gap value has only a moderate influence on the shape of the curve; in the fit it was fixed to 6 meV, corresponding to the upper gap values reported for LiFeAs [11,44–46]. The transition temperature obtained in the fit amounts to $T_C = 13.2(5) \text{ K}$, which is significantly below other values reported for this field. Khim *et al.* [47], for example, found a transition temperature of around 15 K for an applied field of 9 T perpendicular to the c direction. Baek *et al.* [48], however, found evidence of two different transition temperatures. The susceptibility data, measured with different magnetic fields parallel and perpendicular to the c direction, show superconducting transition temperatures which are in agreement with those measured by Khim *et al.* [47], but the NMR Knight-shift data, taken on the same crystal, show lower transition temperatures. The transition temperature Baek *et al.* measured at an applied field of 9 T perpendicular to the c

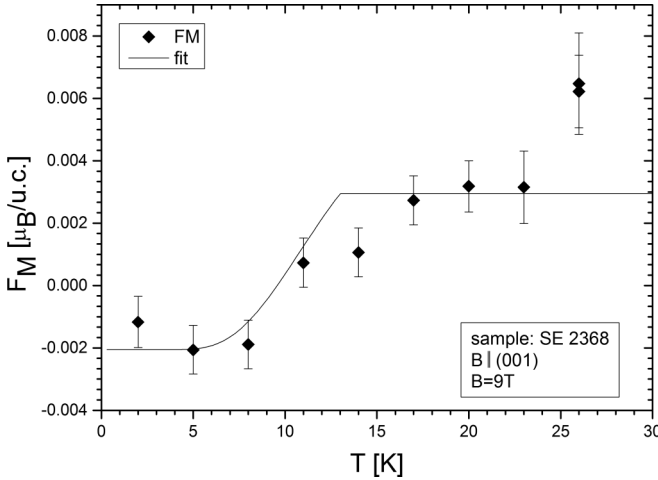


FIG. 2. Magnetic moments of the (110) Bragg reflection with an applied field of 9 T parallel to the c direction. Solid lines are fits of the Yosida function [41].

direction agrees perfectly with our value [48]. Baek *et al.* suggest that there is first a triplet superconducting phase, which changes character to a singlet phase at the lower transition temperature [48]. However, it is also possible that there is first superconducting behavior just on the surface, which cannot be detected by our bulk-sensitive flipping-ratio measurements. Furthermore, there is clear evidence that LiFeAs exhibits different gap values on its different Fermi-surface sheets. A multiband, multigap theory is highly desirable for a more quantitative analysis of the local spin susceptibility in this material.

The results shown in Fig. 1 agree perfectly with those obtained by the same flipping-ratio technique for Co-doped BaFe₂As₂ [35]. Both the magnetization in the normal phase and the suppression of susceptibility in the superconducting state are comparable in both compounds, which disagrees with speculations that stoichiometric LiFeAs is very close to a ferromagnetic instability.

The magnetic moments for an applied field of 9 T parallel to the c direction are shown in Fig. 2. In this field direction we measured only the (110) Bragg reflection with lower statistics because of the limited beam time. The solid line is, again, a fit of the Yosida function (with fixed $T_c = 13$ K), which is consistent with the data, but the low statistics do not allow for an independent determination of the superconducting transition temperature.

We also measured the spin susceptibility for a second sample (SE3027), again applying a magnetic field of 9 T, but parallel to the [100] direction. Here the Bragg reflection (002)

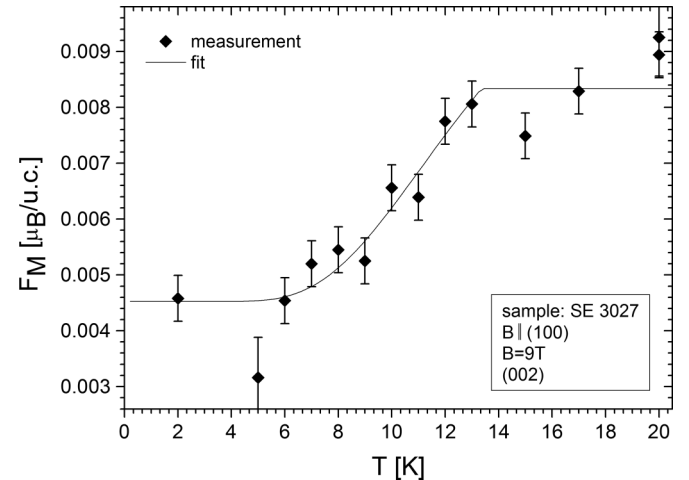


FIG. 3. Magnetic moments of the (002) Bragg reflection with an applied field of 9 T parallel to the [100] direction. The solid line is a fit to the Yosida function [41].

was chosen. The results can again be well described with the Yosida function, as shown in Fig. 3. The fit with the Yosida function yields a transition temperature of $T_c = 13.4(6)$ K, in good agreement with the value obtained for the other in-plane direction of the external field.

III. CONCLUSIONS

In conclusion, we have studied the spin susceptibility in LiFeAs as a function of temperature. For all directions of the external magnetic field, in particular, the one for which a NMR Knight-shift experiment yielded evidence of triplet pairing, we find the drop in spin susceptibility characteristic for a singlet superconductor. However, the drop in spin susceptibility occurs below the onset of superconductivity as observed in ac susceptibility or resistivity measurements. The reduced transition temperature at high field in our experiment nicely agrees with the anomaly in recent Knight-shift experiments, but the reasons for the apparently two transitions require further study.

ACKNOWLEDGMENTS

This work was supported by the Deutsche Forschungsgemeinschaft (DFG) through Sonderforschungsbereich 608 and through Priority Programme SPP1458 (Grant Nos. BE1749/13, BU887/15-1, and BR2211/1-1). S.W. thanks the DFG for funding through the Emmy Noether Programme (Project No. 595/3-1).

-
- [1] Y. Kamihara, T. Watanabe, M. Hirano, and H. Hosono, *Am. Chem. Soc.* **130**, 3296 (2008).
 - [2] X. H. Chen, T. Wu, G. Wu, R. H. Liu, H. Chen, and D. F. Fang, *Nature* **453**, 761 (2008).
 - [3] H. Takahashi, K. Igawa, K. Arii, Y. Kamihara, M. Hirano, and H. Hosono, *Nature* **453**, 376 (2008).
 - [4] P. Hirschfeld, M. M. Korshunov, and I. I. Mazin, *Rep. Prog. Phys.* **74**, 124508 (2011).
 - [5] H. Luetkens, H.-H. Klauss, R. Khasanov, A. Amato, R. Klingeler, I. Hellmann, N. Leps, A. Kondrat, C. Hess, A. Köhler *et al.*, *Phys. Rev. Lett.* **101**, 097009 (2008).
 - [6] H. Luetkens, H.-H. Klauss, M. Kraken, F. J. Litterst, T. Dellmann, R. Klingeler, C. Hess, R. Khasanov, A. Amato, C. Baines *et al.*, *Nat. Mater.* **8**, 305 (2009).

- [7] M. A. McGuire, A. D. Christianson, A. S. Sefat, B. C. Sales, M. D. Lumsden, R. Jin, E. A. Payzant, D. Mandrus, Y. Luan, V. Keppens *et al.*, *Phys. Rev. B* **78**, 094517 (2008).
- [8] J. H. Tapp, Z. Tang, B. Lv, K. Sasnal, B. Lorenz, P. C. W. Chu, and A. M. Guloy, *Phys. Rev. B* **78**, 060505 (2008).
- [9] X. C. Wang, Q. Liu, Y. Lv, W. Gao, L. X. Yang, R. Yu, F. Y. Li, and C. Jin, *Solid State Commun.* **148**, 538 (2008).
- [10] M. J. Pitcher, D. R. Parker, P. Adamson, S. J. C. Herkelrath, A. T. Boothroyd, R. M. Ibberson, M. Brunelli, and S. J. Clarke, *Chem. Commun.* **2008**, 5918 (2008).
- [11] S. V. Borisenko, V. B. Zabolotnyy, D. V. Evtushinsky, T. K. Kim, I. V. Morozov, A. N. Yaresko, A. A. Kordyuk, G. Behr, A. Vasiliev, R. Follath *et al.*, *Phys. Rev. Lett.* **105**, 067002 (2010).
- [12] G. Lee, H. S. Ji, Y. Kim, C. Kim, K. Haule, G. Kotliar, B. Lee, S. Khim, K. H. Kim, K. S. Kim, K.-S. Kim, and J. H. Shim, *Phys. Rev. Lett.* **109**, 177001 (2012).
- [13] C. Putzke, A. I. Coldea, I. Guillamón, D. Vignolles, A. McCollam, D. LeBoeuf, M. D. Watson, I. I. Mazin, S. Kasahara, T. Terashima, T. Shibauchi, Y. Matsuda, and A. Carrington, *Phys. Rev. Lett.* **108**, 047002 (2012).
- [14] B. Zeng, D. Watanabe, Q. R. Zhang, G. Li, T. Besara, T. Siegrist, L. Y. Xing, X. C. Wang, C. Q. Jin, P. Goswami, M. D. Johannes, and L. Balicas, *Phys. Rev. B* **88**, 144518 (2013).
- [15] J. Ferber, K. Foyevtsova, R. Valentí, and H. O. Jeschke, *Phys. Rev. B* **85**, 094505 (2012).
- [16] N. Qureshi, P. Steffens, Y. Drees, A. C. Komarek, D. Lamago, Y. Sidis, L. Harnagea, H. J. Grafe, S. Wurmehl, B. Büchner, and M. Braden, *Phys. Rev. Lett.* **108**, 117001 (2012).
- [17] A. N. Yaresko, G.-Q. Liu, V. N. Antonov, and O. K. Andersen, *Phys. Rev. B* **79**, 144421 (2009).
- [18] C. Lester, J.-H. Chu, J. G. Analytis, T. G. Perring, I. R. Fisher, and S. M. Hayden, *Phys. Rev. B* **81**, 064505 (2010); H.-F. Li, C. Broholm, D. Vaknin, R. M. Fernandes, D. L. Abernathy, M. B. Stone, D. K. Pratt, W. Tian, Y. Qiu, N. Ni, S. O. Diallo, J. L. Zarestky, S. L. Bud'ko, P. C. Canfield, and R. J. McQueeney, *ibid.* **82**, 140503(R) (2010).
- [19] X. Wang, Q. Liu, Y. LV, Z. Deng, K. Zhao, R. Yu, J. Zhu, and C. Jin, *Science China Phys. Mech. Astron.* **53**, 1199 (2010).
- [20] S. Wurmehl *et al.* (unpublished).
- [21] J. D. Wright, M. J. Pitcher, W. Trevelyan-Thomas, T. Lancaster, P. J. Baker, F. L. Pratt, S. J. Clarke, and S. J. Blundell, *Phys. Rev. B* **88**, 060401 (2013).
- [22] S. Baek, H. Grafe, F. Hammerath, M. Fuchs, C. Rudisch, L. Harnagea, S. Aswartham, S. Wurmehl, J. van den Brink, and B. Büchner, *Eur. Phys. J. B Condens. Matter Complex Syst.* **85**, 1 (2012).
- [23] T. Hänke, S. Sykora, R. Schlegel, D. Baumann, L. Harnagea, S. Wurmehl, M. Daghofer, B. Büchner, J. van den Brink, and C. Hess, *Phys. Rev. Lett.* **108**, 127001 (2012).
- [24] P. M. R. Brydon, M. Daghofer, C. Timm, and J. van den Brink, *Phys. Rev. B* **83**, 060501(R) (2011).
- [25] A. Aperis and G. Varelogiannis, *arXiv:1303.2231*.
- [26] J. A. Duffy, S. M. Hayden, Y. Maeno, Z. Mao, J. Kulda, and G. J. McIntyre, *Phys. Rev. Lett.* **85**, 5412 (2000).
- [27] A. P. Mackenzie and Y. Maeno, *Rev. Mod. Phys.* **75**, 657 (2003).
- [28] C. G. Shull and F. A. Wedgwood, *Phys. Rev. Lett.* **16**, 513 (1966).
- [29] C. Stassis, J. Arthur, C. F. Majkrzak, J. D. Axe, B. Batlogg, J. Remeika, Z. Fisk, J. L. Smith, and A. S. Edelstein, *Phys. Rev. B* **34**, 4382 (1986).
- [30] J. Boucherle, J. Henry, R. J. Papoulier, J. Rossat-Mignod, J. Schweizer, F. Tasset, and G. Uimin, *Physica B* **192**, 25 (1993).
- [31] H.-J. Grafe, D. Paar, G. Lang, N. J. Curro, G. Behr, J. Werner, J. Hamann-Borrero, C. Hess, N. Leps, R. Klingeler, and B. Büchner, *Phys. Rev. Lett.* **101**, 047003 (2008).
- [32] Y. Nakai, K. Ishida, Y. Kamihara, M. Hirano, and H. Hosono, *J. Phys. Soc. Jpn.* **77**, 073701 (2008).
- [33] T. Imai, K. Ahilan, F. Ning, M. A. McGuire, A. S. Sefat, R. Jin, B. C. Sales, and D. Mandrus, *J. Phys. Soc. Jpn. Suppl. C* **77**, 47 (2008).
- [34] F. Ning, K. Ahilan, T. Imai, A. S. Sefat, R. Jin, M. A. McGuire, B. Sales, and D. Mandrus, *J. Phys. Soc. Jpn.* **78**, 013711 (2009).
- [35] C. Lester, J.-H. Chu, J. G. Analytis, A. Stunault, I. R. Fisher, and S. M. Hayden, *Phys. Rev. B* **84**, 134514 (2011).
- [36] I. Morozov, A. Boltalin, O. Volkova, A. Vasiliev, O. Kataeva, U. Stockert, M. Abdel-Hafiez, D. Bombor, A. Bachmann, L. Harnagea *et al.*, *Crystal Growth Design* **10**, 4428 (2010).
- [37] M. Braden, P. Schweiss, G. Heger, W. Reichardt, Z. Fisk, K. Gamayunov, I. Tanaka, and H. Kojima, *Physica C* **223**, 396 (1994).
- [38] P. Steffens, C. H. Lee, N. Qureshi, K. Kihou, A. Iyo, H. Eisaki, and M. Braden, *Phys. Rev. Lett.* **110**, 137001 (2013).
- [39] P. Coppens, Z. Su, and P. Becker, *International Tables of Crystallography, Vol. C: Analysis of Charge and Spin Densities* (Kluwer Academic, New York, 2004).
- [40] J. Schweizer, in *Neutron Scattering from Magnetic Materials*, edited by T. Chatterji (Elsevier B.V., Amsterdam, 2006).
- [41] K. Yosida, *Phys. Rev.* **110**, 769 (1958).
- [42] D. Einzel, *J. Low Temp. Phys.* **130**, 493 (2003).
- [43] A. M. Clogston, A. C. Gossard, V. Jaccarino, and Y. Yafet, *Phys. Rev. Lett.* **9**, 262 (1962).
- [44] T. Hanaguri, K. Kitagawa, K. Matsubayashi, Y. Mazaki, Y. Uwatoko, and H. Takagi, *Phys. Rev. B* **85**, 214505 (2012).
- [45] S. Chi, S. Grothe, R. Liang, P. Dosanjh, W. N. Hardy, S. A. Burke, D. A. Bonn, and Y. Pennec, *Phys. Rev. Lett.* **109**, 087002 (2012).
- [46] K. Umezawa, Y. Li, H. Miao, K. Nakayama, Z.-H. Liu, P. Richard, T. Sato, J. B. He, D.-M. Wang, G. F. Chen, H. Ding, T. Takahashi, and S.-C. Wang, *Phys. Rev. Lett.* **108**, 037002 (2012).
- [47] S. Khim, B. Lee, J. W. Kim, E. S. Choi, G. R. Stewart, and K. H. Kim, *Phys. Rev. B* **84**, 104502 (2011).
- [48] S.-H. Baek, L. Harnagea, S. Wurmehl, B. Büchner, and H.-J. Grafe, *J. Phys.: Condens. Matter* **25**, 162204 (2013).